Available online at www.sciencedirect.com
SCIENCE DIRECT®
International Journal of Thermal Sciences 43 (2004) 1091–1100
International Journal of Thermal Sciences
www.elsevier.com/locate/ijts

Development of flat-plate thermal and velocity boundary layers under highly turbulent and instable air flows: Reynolds numbers ranging from 8400 to 127 000

Alain Kondjoyan [a,*], Frédéric Péneau [b], Henri-Claude Boisson [c]

[a] *Institut national de la recherche agronomique, S.R.V., 63122 St Genès Champanelle, France*
[b] *CERAM, Euro-American Institute of Technology, 157, rue A. Einstein, 06902 Sophia Antipolis cédex, France*
[c] *Institut de mécanique des fluides de Toulouse, al. Prof. Camille Soula, 31400 Toulouse, France*

Received 11 December 2002; received in revised form 6 October 2003; accepted 24 February 2004

Available online 24 June 2004

Abstract

Temperature and velocity profiles were measured in a flat-plate boundary layer subjected to free stream turbulence intensities ranging from 1 to 50% and at Reynolds numbers from 8 400 to 127 000. The greatest turbulence intensity values were accompanied by large scales instabilities into the flow. When $Tu_\infty \approx 1\%$ the temperature and velocity profiles were in agreement with the Blasius solution providing that the real boundary layer thickness was taken into account. For $Tu_\infty \geqslant 6\%$ the thermal and velocity boundary layers greatly thickened as well as the displacement and momentum thicknesses. A "wake region" was observed in the profiles and there was an increase of slopes in the near-wall region of the thermal profiles. Moreover turbulent energy was produced in the boundary layer. Some differences were observed between the thermal and velocity boundary layers which can be explained by the unheated starting length which existed at the leading edge of the plate.

Keywords: Plate boundary-layer transfer heat air turbulence

1. Introduction

Numerous industrial situations involve frictions and heat transfers between solids and air flows whose velocities are moderate but which are highly turbulent. This is particularly the case during chemical and food processes when air flows from fans are used as a thermal medium for drying, cooling, heating or cooking products. The effect of free stream turbulence intensity on transfers around cylinders, spheres or other bodies of even more complex shapes has been widely studied and was shown to be very important. Works prior to 1994 on the effect of turbulence on transfer coefficient around sphere and cylinders have been reviewed by the authors [1]. They have also performed additional experiments to analyse the effect of highly turbulent flows on transfers coefficients at the surface of cylinders and of bodies of more complex shapes [2–4]. As regards flat plates, 50 experimental studies have been reviewed in details by the authors in a previous paper [5].

When the boundary layer is already fully turbulent ($Re_x > 5 \times 10^5$), an increase in free stream turbulence leads to an important increase in the heat transfer and skin friction coefficients with a greater effect on the heat transfer coefficient. Free stream turbulence also modifies the velocity and temperature profiles in the boundary layer especially in the "wake region" of the profiles [6–12]. This phenomenon mainly results from the free-stream turbulence intensity even if the effect of the turbulence integral scale cannot be neglected.

The effect of free-stream turbulence on a flat-plate boundary layer at moderate Reynolds numbers ($Re_x < 2 \times 10^5$) has been studied very little. Some results have been obtained by Kestin et al. [13] and Junkhan and Serovy [14] which show that the heat transfer coefficient tends to increase with free stream turbulence. But these results are contradictory and re-

* Corresponding author. Fax: +33-4-73-62-40-89.
E-mail addresses: alain.kondjoyan@clermont.inra.fr (A. Kondjoyan), frederic.peneau@cote-azur.cci.fr (F. Péneau), boisson@imft.fr (H.-C. Boisson).

1290-0729/$ – see front matter
doi:10.1016/j.ijthermalsci.2004.02.024

Nomenclature

L	turbulent integral scale	m
Nu	Nusselt number, $= h \cdot x/\lambda$	
Pr	Prandtl number	
Re_x	Reynolds number based on $X = U \cdot X/\nu$	
Tu	turbulence intensity in the main stream direction: u'/U_∞	
U	air velocity in the main stream direction	$\mathrm{m{\cdot}s^{-1}}$
u	velocity fluctuation in the main stream direction	$\mathrm{m{\cdot}s^{-1}}$
u'	rms velocity fluctuation in the main stream direction, $= \sqrt{\overline{u^2}}$	$\mathrm{m{\cdot}s^{-1}}$
X	distance from the plate leading edge	m
y	transverse coordinate in the direction normal to the wall	m
z	coordinate in the spanwise direction	m

Greek symbols

δ_V	velocity boundary layer thickness, i.e., distance from the plate surface at which	
δ_t	thermal boundary layer thickness	m
δ^*	boundary layer displacement thickness	m
δ^{**}	boundary layer momentum thickness	m
Φ_g	Hole diameter of turbulent promoters	m
λ	thermal conductivity of air	$\mathrm{W{\cdot}m^{-1}{\cdot}K^{-1}}$
σ_g	perforated area of turbulent promoters	
η	normalised distance perpendicular to the wall, $= y/\delta$	
ν	kinematic viscosity of air	$\mathrm{m^2{\cdot}s^{-1}}$
ξ	unheated starting length of the plate	m

Subscript

∞	free stream condition

stricted to very small turbulence intensities ($Tu_\infty \leqslant 3$–6%). To our knowledge, higher turbulence intensities have only been investigated experimentally by Dyban and Epik [15]. Results, obtain in a velocity boundary layer in the range: $6000 < Re_x < 50\,000$ and $Tu_\infty \leqslant 25\%$, show that a wake region appears in the outer part of the boundary layer profile when free stream turbulence increases. A maximum value is also observed in the profile of the velocity fluctuation.

Mechanisms responsible for earlier transition or bypass transition due to free stream disturbances are still not fully known. Current knowledge of the receptivity of the velocity boundary-layer to these external disturbances has been reviewed recently [16]. Agreement between theory and experiment are excellent when disturbances are created by sound waves or two-dimensional surface roughness. But receptivity to free stream turbulence remains difficult to understand because of the strong three-dimensional nature of the initial disturbances and of the subsequent nonlinear development of the resulting Tollmien–Schilchting waves.

The present study aims at describing the effect of highly turbulent air flows on the development of a boundary layer for Reynolds numbers less than 1.5×10^5. The range of free stream turbulence is wider than in Dyban and Epik's study and both temperature and velocity profiles are measured. Another work was carried out simultaneously by authors using large eddy simulation to better understand the effect of turbulence on heat transfers [17].

2. Materials and methods

A flat plate was located inside the test chamber of a wind tunnel and subjected to air flows of different turbulence intensities or integral length scales. In a first set of experiments, the average velocity and fluctuated velocity profiles were measured in the boundary layer which developed along the surface of the plate. In another set of experiments the surface of the plate was uniformly heated and temperature profiles were measured inside the boundary layer under the same free stream turbulent conditions as previously.

The installation was a 12 m long and 4 m high closed-loop wind tunnel which has already been described in detail in other papers [2,3]. The ratio of the contraction area between the settling chamber and the test section was 9. The residual free stream turbulence intensity inside the test chamber (0.8 m × 0.8 m × 1.60 m) was about 1%. To promote turbulence, different perforated plates were located normal to the air flow in one of the two drawers located upstream of the test chamber.

The flat plate used to study the development of the boundary layer was 1.12 m long, 0.80 m wide and 0.02 m thick. It was located halfway up the test chamber and 0.40 m downstream from its start. Its leading edge was elliptical (major to minor axis ratio of 4) and it was grooved in its middle-width to receive another aluminium plate (0.98 m × 0.10 m × 0.02 m). Top surfaces of the aluminium plate and of the main flat plate were carefully reamed to ensure a perfect smooth transition between the two pieces. Three flat thermal ribbons (of 304.8 mm × 69.9 mm × 2 mm each, electrical resistance 35.4 Ohms) were stuck in line, using a glue with a high thermal conductivity, at the bottom of the aluminium plate. These ribbons were electrically connected in series to an electrical generator and thermally isolated at their bottom using 0.02 m of cork.

The average flow velocity and fluctuations were measured using a constant temperature hot wire anemometer. The hot wire element (5 μm in diameter and 1.25 mm in length) was located between two prongs which were themselves connected to a support. Characterisation of the tur-

bulence downstream of the promoters was performed using a straight prong probe (DANTEC, 55P11) while measurements inside the boundary layer were performed using an "offset" prong probe (DANTEC, 55P15). Repeated calibrations of the response of the hot wire system with respect to air temperature ensured that the absolute error on the velocity measurements was less than $+/-0.1$ m·s^{-1}. The sampling frequency and duration for acquiring the velocity signal were increased as the flow became more turbulent. Sampling frequency ranged between 2 kHz and 10 kHz and recording duration from 1 to 5 s depending on the turbulent conditions.

For thermal experiments, temperature profiles inside the boundary layer were measured using a thermocouple 0.2 mm in diameter connected to a data logging system. The thermocouple was carefully calibrated before each experiment with an error of $+/-0.1\,^{\circ}$C.

A three-axis traversing system made it possible to displace the probe automatically (hot wire or thermocouple) in an area of chosen dimension and location with a pre-selected displacement step. The displacement step could be theoretically as small as 0.01 mm. The probe location and response were recorded using a computer linked to the system.

The nature of the turbulence downstream of a perforated plate cannot be determined theoretically but is known to depend on the plate perforation diameter Φ_g and on the promoter perforated area, σ_g (expressed as a percentage of the plate area). At a given distance from the promoter, when the jets created by perforations have sufficiently mixed together the turbulence becomes nearly homogeneous and isotropic. Then the intensity of turbulence decreases exponentially with the distance from the promoter. The aim of this study was to generate successively values of free stream turbulence intensity between 1% and more than 20%. Each level of Tu_∞ had also to remain nearly constant in the flow direction all along the flat plate. To reach this goal, perforated plates with different values of Φ_g and σ_g were chosen using previous studies [2,3,18]. Turbulence intensities of about 6, 12 and 40% were obtained along the test chamber using plates whose characteristics and location are given in Table 1. Plates perforations were circular and aligned regularly in lines and columns for plates (1), (2) and (3) located downstream of the wind-tunnel contraction. On plate (4) perforations were located on four concentric circles and one perforation was located at the centre of the plate. The distance between the turbulence promoters and the leading edge of the plate used for boundary layer measurements was 0.45 m for promoters (1), (2) or (3) and 2.45 m for promoter (4).

Downstream of plates (1), (2) and (4) the average velocity was uniform in every cross-section of the test chamber. The free stream turbulence was a decaying turbulence. The ratio of the longitudinal component to the transverse component of the velocity fluctuation has been measured in previous studies downstream of promoters (1), (2) and (4) in several points along the experimental chamber using in addition to the 90°-wire probe a single rotated 45°-wire probe [2, 18]. This ratio ranged from 0.8 to 1.2 depending on the promoter which is require (but not sufficient) for a flow turbulence to be isotropic. Free stream turbulence intensity decreased exponentially with the distance to the promoters 1, 2 and 4. The length of the flat plate used for the boundary layer measurements was located in an area corresponding to the plateaus of these decreasing curves. Details on the flow downstream promoters (1), (2) and (4) and relations which make it possible to connect the different turbulent scales are given in references [2,18]. Only the extreme values of these plateaus are given in Table 1. The procedure used to determine the turbulence integral length scales from turbulent spectra downstream of promoter (1), (2) and (4) are detailed in reference [18]. The use of two different turbulence promoters (2) and (4) (located either upstream or downstream of the contraction area) to obtain a free stream turbulence intensity of 12% made it possible to reach different turbulent scales in the test chamber under a similar value of Tu_∞.

Downstream of promoter (3) the turbulent flow was not fully uniform neither was it steady because the flat plate was located in a region where jets had not finished to mix together. Thus spatial differences in average velocity still existed in the cross-flow direction and along the flat plate. In this case, the calculated Tu_∞ did not represent a well-defined value of the free stream turbulence intensity. It only gave information on the level of the turbulent fluctuation in the flow direction. The signal of the fluctuation was recorded and averaged until the ratio u'/U became stable. Records of the fluctuations on short durations showed that the main part of the average u' came from rapid fluctuations comparable to those originated from promoters (1), (2) and (4). However larger scale instabilities were also inevitably included in

Table 1
Characteristics and locations of the perforated plates used to promote turbulence. Free stream turbulence intensity and integral scale measured at $X = 0.06$ and 0.90 m

N° and location of the promoter	φ_g [mm]	σ_g [%]	Free stream turbulence				Flow characteristics
			$X = 0.06$ m		$X = 0.90$ m		
			Tu_∞ [%]	L [m]	Tu_∞ [%]	L [m]	
(1) Downstream contraction	18	46	6	0.015	3	0.027	Homogeneous and isotropic
(2) Downstream contraction	45	46	16	0.040	11	0.080	Nearly homogeneous and isotropic
(3) Downstream contraction	100	19	35	?	50	?	Unsteady
(4) Upstream contraction	154	9	14	0.100	10	0.100	Nearly homogeneous and isotropic

the calculations of Tu_∞. Even if the flow downstream of promoter (3) was not as well defined as those encountered downstream of promoters (1), (2) and (4), it was probably closer to most of the flows encountered in industrial plants. Promoter (3) was used to see if results obtained under $Tu_\infty \leqslant$ 12% can be extended to practical situations.

The measurement of a velocity profile began by installing the chosen turbulent promoter inside the wind tunnel drawer. The fan speed was fixed to reach an average air velocity of about 2.0 m·s^{-1} inside the test chamber (this air velocity was measured accurately afterwards). Turbulence intensity and integral scale of the free stream flow were determined. The traversing system was reset to zero in the flow direction (X) by conveying the tip of the hot wire prongs on a line perpendicular to the flat plate surface and which crossed the stagnation point of the plate leading edge. Then the probe was conveyed at the middle-width of the plate (spanwise direction Z) and at a given distance X of either 0.06, 0.14, 0.30 or 0.90 m from the leading edge of the plate. The hot wire prongs were brought into contact with the plate wall, and the traversing system was reset to zero in the direction perpendicular to the plate surface (Y). A telescope ($\times 24$) was used to accurately locate the point of contact (error of this visual observation through the magnifying glass was $+/-0.05$ mm). From the point of contact upward the air velocity and fluctuation in the main flow direction were measured every 0.1 mm until the frontier of the boundary layer was reached (average velocity value became constant).

Before measuring a temperature profile, the aluminium part of the flat plate was heated by delivering an electrical current of about 0.30 A through electrical ribbons. The intensity of the electrical current in fact depended on the turbulence conditions and was fixed to obtain a difference in temperature between the flow and the plate surface of about 2.0 °C. This difference was sufficiently large to minimize the error on temperature measurements and sufficiently small to avoid the heating of the plate introducing fluctuations in the controlled wind tunnel temperature. After these conditions were set, several hours had to be waited for to reach a perfect steady state equilibrium. The traversing system was reset to zero in the x and y direction and the average temperature was measured every 0.1 mm from the plate wall upward as for the velocity measurements. At each distance y from the wall the average temperature was calculated from 25 measurements performed during 5 seconds. The wall and free stream temperatures were measured using the same thermocouple located either at the wall or outside the boundary layer. Temperature profiles were measured at more locations X than the velocity profiles, i.e., at 0.06 m, 0.10, 0.14, 0.20, 0.40, 0.60 and 0.90 m from the plate leading edge.

3. Results

Velocity measurements using hot-wires are known to be erroneous very close to the wall because of the influence of thermal exchanges by conduction and radiation between the wall and the wire [19]. When moving away from the wall, the velocity seems to decrease to a minimum and then to increase again. The existence of this minimum is well known to be a failure of hot wire anemometry in the vicinity of the wall and is impossible to avoid even when decreasing the temperature of the wire. Different methods of correction have been proposed in the literature but they are very specific to the measuring conditions (wall material, air velocity range, overheat ratio …) and do not take into account radiation exchanges [19]. In our case, the corrections proposed by the literature did not fully correct the near-wall non-physical variation. Thus the points located before and the first point located just after the non-physical minimum were simply removed from the raw profiles (Fig. 1). As this false minimum existed whatever the free stream turbulence intensity, the same criterion was applied to all cases.

Then the raw profiles measured every 0.1 mm step were most of the time smoothed by averaging each measuring

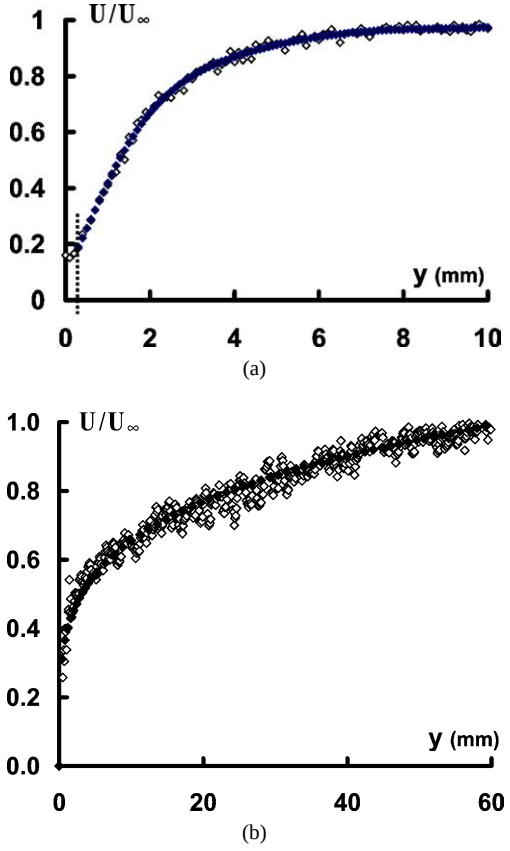

Fig. 1. Comparison between the raw velocity profile (white diamonds) and the treated profile (black diamonds): (a) Typical profile obtained for $Tu_\infty \leqslant 12\%$, experimental points located left from the dashed line have been removed, (b) $Tu_\infty \approx 50\%$, $Re_x = 126\,900$ in this case the experimental points were the more scattered.

point with the three-to-five following ones (no smoothing or little smoothing was used when the boundary layer was very thin, $X = 0.06$ m). Fig. 1(a) compares typical raw and smoothed profiles obtained downstream of turbulence promoters 1, 2 or 4. The average difference between the smoothed values and the experimental values is equal to 3% of the experimental value and it never exceeds 5% (Fig. 1(a)).

Downstream of promoter (3) profiles (mainly the velocity profiles) remained noisy despite the previous average smoothing. In this case, a further polynomial smoothing was applied. Raw data and two step smoothed data are given in Fig. 1(b). The smoothed profile gives a faithful rendering of the shape of the raw data profile. The average difference between the smoothed values and the experimental values is 7% of the experimental value. However differences of 15% can be observed locally.

3.1. Free stream turbulence intensity of about 1%

The thickness of the velocity boundary layer at the different locations X was determined from the velocity profiles ($U = 0.99U_\infty$). Values were compared to the thickness of a laminar boundary layer which would have started at the leading edge of the plate. The present velocity boundary layer obtained under $Tu_\infty \approx 1\%$ was about 10–15% thicker than the theoretical laminar boundary layer.

The ratio of the thermal-to-velocity boundary layer thickness $\delta t/\delta v$ for a thermal boundary layer which develops on a flat plate with an unheated starting length can be calculated from [20]:

$$\frac{\delta_t}{\delta_v} = \frac{Pr^{-1/3}}{1.026}\left[1 - \left(\frac{\xi}{X}\right)^{3/4}\right]^{1/3} \tag{1}$$

where ξ is the length of the unheated starting length which was 0.04 m in our case.

Thermal boundary layer thickness determined from the temperature profiles ($T - T_s = 0.99(T_\infty - T_s)$) for $Tu_\infty = 1\%$ at different locations X was less than 5% different from the values calculated from (1). Because of the unheated starting length, the thermal boundary layer at $X = 0.06$ m was much thinner than the velocity boundary layer. However, in air ($Pr = 0.7$), thermal boundary layers thicken faster than velocity boundary layers. Hence as soon as $X \geqslant 0.50$ m, the thickness of the two boundary layers was of the same order.

Profiles measured in the thermal and velocity boundary layers at $X = 0.06$ m ($Re_x = 8460$) and $X = 0.90$ m ($Re_x = 126\,900$) are shown in normalised coordinates in Fig. 2. The

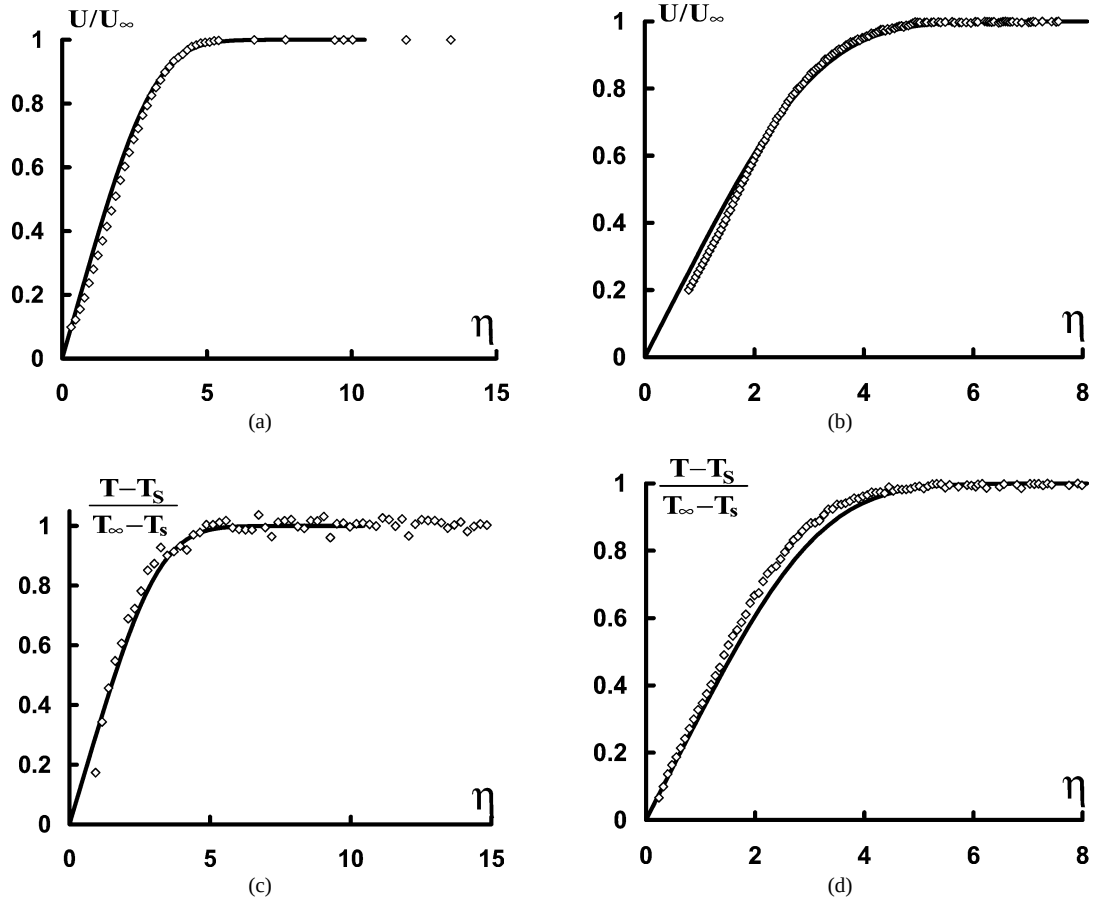

Fig. 2. Comparison of the velocity and temperature profiles for $Tu_\infty \approx 1\%$ with the solution of Blasius (full line): (a) velocity profile, $X = 0.06$ m ($Re_x = 8460$); (b) velocity profile, $X = 0.90$ m ($Re_x = 126\,900$); (c) temperature profile, $X = 0.06$ m ($Re_x = 8460$), (d) temperature profile, $X = 0.90$ m ($Re_x = 126\,900$).

value of δ_v or δ_t used to calculate η is the real thickness of the thermal or of the velocity boundary layers measured at the location X. Comparison with the Blasius theoretical profile shows that these measured average profiles are very close to those of a laminar boundary layer.

3.2. Modification of the average velocity profile with turbulence

Mean velocity profiles measured in the boundary layer at $X = 0.30$ m ($Re_x = 42\,300$) and $X = 0.9$ m ($Re_x = 126\,900$) for the different free stream turbulence intensities are shown in Fig. 3(a) and (b). As previously noticed by Dyban and Epik [15], the increase in turbulence intensity modifies the part of the boundary layer which is in contact with the free stream. This part of the profile becomes progressively "similar" to the "wake region" of a fully turbulent boundary layer. This phenomenon is more striking here than in the experiments of Dyban and Epik and begins as soon as $Re_x = 8460$ and $Tu_\infty = 6\%$. It becomes all the more pronounced as the free stream turbulence intensity and Reynolds number increase.

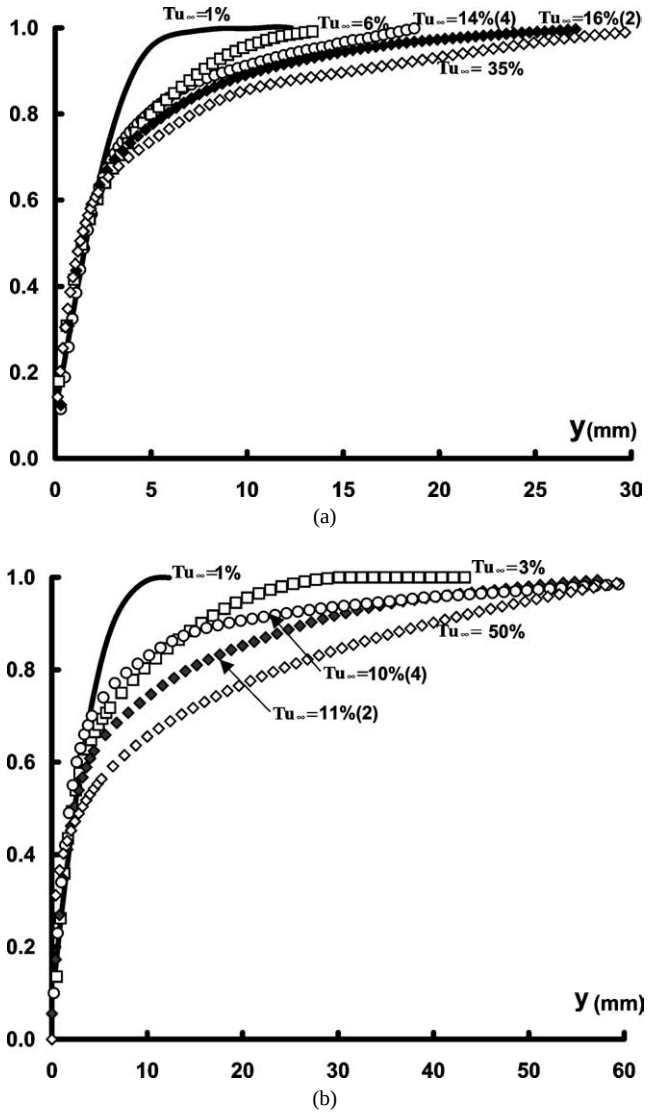

Fig. 3. Evolution of the velocity profile with Tu_∞ at: (a) $X = 0.30$ m ($Re_x = 42\,300$), (b) $X = 0.90$ m ($Re_x = 126\,900$). Full line, $Tu_\infty = 1\%$; white squares, $Tu_\infty = 6$–3%; white dots, $Tu_\infty = 14$–10%, promoter N°4 upstream contraction area; black diamonds, $Tu_\infty = 16$–11%, promoter N°2 downstream contraction area, white diamonds, $Tu_\infty = 35$–50%.

For $Tu_\infty \approx 12\%$ profiles measured downstream of the two different promoters are about the same (the small discrepancy can be explained by the difference in Tu_∞) when $Re_x = 42\,300$ and very different for $Re_x = 126\,900$. Hence the wake region of the profile is affected by the turbulent scale but only when the boundary layer becomes thick.

For $Tu_\infty \approx 50\%$ and $Re_x = 126\,900$, the velocity profile is very different from the Blasius profile and measurements can be described using a power law [21]:

$$\frac{U}{U_\infty} = \left(\frac{y}{\delta}\right)^{1/n} \tag{2}$$

Exponent n is 4.4 and thus much lower than the value of 7.0 generally admitted for a fully turbulent boundary layer [21]. Moreover the power law overestimates the values measured in the near-wall region (for $U/U_\infty < 0.4$).

The appearance of a "wake region" in the velocity profile under free stream turbulence is accompanied by a large increase in the thickness of the boundary layer (Fig. 4(a)). When $Tu_\infty \approx 1\%$, experimental thickness is close to Blasius solution. An increase in free stream turbulence from 1 to 6% leads to a considerable thickening of the boundary layer which is more pronounced for a further variation of Tu_∞ from 6 to 12%. For $Tu_\infty \leqslant 12\%$ the thickening of the boundary layer is proportional to Re_x. Beyond $Tu_\infty = 12\%$, the effect of Tu_∞ is less pronounced and is mainly observed for values or Re_x lower than 30 000 (i.e., near the leading edge of the flat plate).

When the boundary layer is fully laminar or on the contrary fully turbulent, the thickness to the distance X ratio is described by the following equation:

$$\frac{\delta_v}{X} = A\,Re_x^{-n} \tag{3}$$

A and n are equal to 5.0, 0.5 and 0.37, 0.2 for the laminar and turbulent boundary layer respectively [21]. Ratios δ_v/x make it possible to compare the results obtained at different locations on the plate and under different air velocities. Experimental values of δ_v/x measured under different free stream turbulence intensities are presented as a function of Re_x in Fig. 4(b). When $Tu_\infty = 6\%$ experimental results can be fitted using relation (3) with a value of n close to 0.5. On the contrary, when $Tu_\infty > 12\%$, the value δ_v/x, which is very important for $Re_x = 8460$, decreases very fast downstream. Relation (3) does not fit the experimental results well and parameters admitted for a fully turbulent boundary layer ($A = 0.37$, $n = 0.2$) cannot be used.

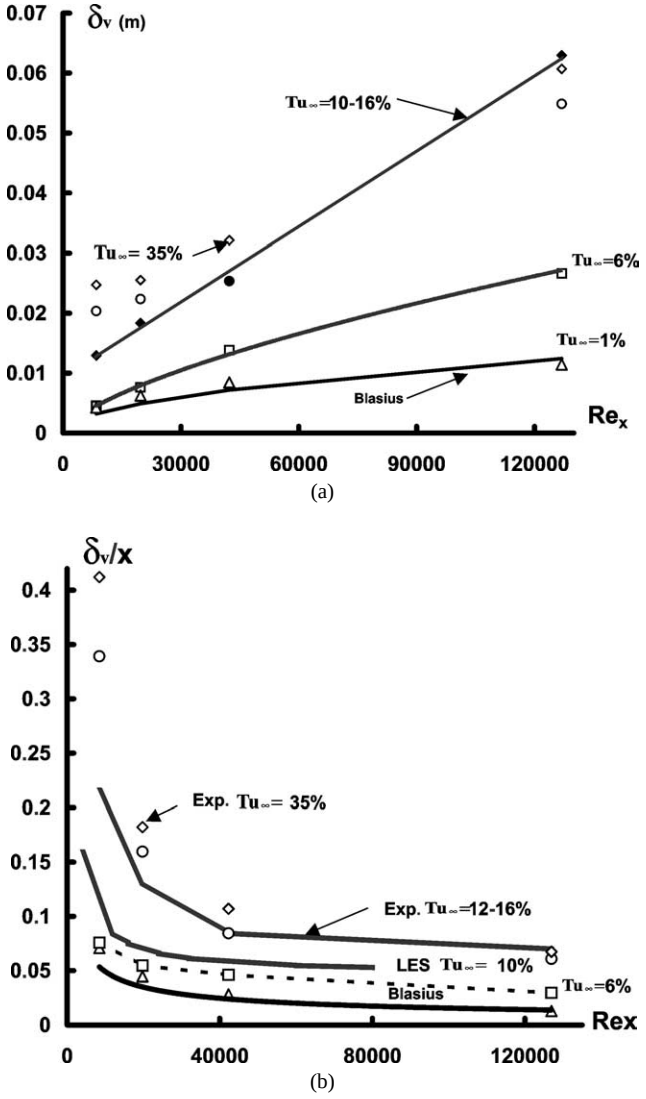

Fig. 4. Variation of the velocity boundary layer thickness with Tu_∞: (a) δ_v as a function of Re_x, (b) δ_v/x as a function of Re_x. Symbols are the same as in Fig. 2. Comparison of the present experimental results with results calculated by Péneau et al. for $U_\infty = 1.23$ m·s^{-1} and $Tu_\infty = 10\%$ using Large Eddy Simulation [9].

The present results can be compared to those calculated by Péneau et al. [17] using Large Eddy Simulations for an air velocity of 1.23 m·s^{-1} and a turbulence intensity of 10% (Fig. 4(b)). Péneau's results are consistently located in between present experimental results obtained for $Tu_\infty = 6\%$ and for $Tu_\infty \approx 12\%$. However the thickening of the velocity boundary layer especially near the plate leading edge, seems to be slightly greater in this study than in the large eddy simulations.

The displacement δ^* and momentum δ^{**} thicknesses also increase with free stream turbulence intensity. A very large increase of δ^{**} is particularly observed for a variation of Tu_∞ from 6% to about 12% (Fig. 5). However, contrary to what was observed for δ_v, displacement and momentum thicknesses go on increasing for $Tu_\infty > 12\%$ and $Re_x =$

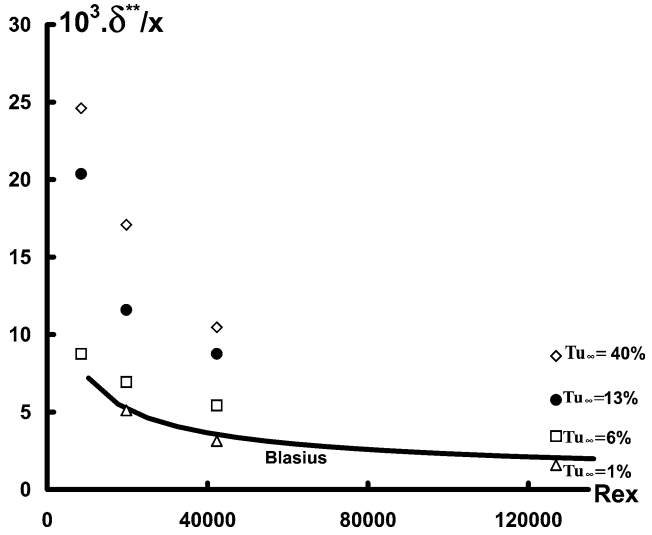

Fig. 5. Variation of the velocity boundary layer momentum thickness δ^{**}/x with Tu_∞. Black dots represent the mean results obtained for Tu_∞ in between 12 and 16% with the two types of turbulence promoters N°2 and 4. Other symbols are the same as in Figs. 2 and 3.

40 000–120 000 even if the variation is less pronounced. The shape factor δ^*/δ^{**} which is close to the Blasius solution 2.59 when $Tu_\infty = 1\%$, decreases with Tu_∞ and reaches 1.4–1.5 when $Tu_\infty > 12\%$ and $Re_x > 40\,000$. This remains above the value of the shape factor ($\delta^*/\delta^{**} = 1.28$) generally admitted for a fully turbulent boundary layer.

The thickening of the velocity boundary layer with Tu_∞ is accompanied by a slight increase of the profile slope in the near wall region. This increase of slope is much less pronounced than in the experiments of Dyban and Epik [5, 15] and falls into the range of our experimental errors.

3.3. Modification of the mean temperature profile with turbulence

Mean temperature profiles measured inside the boundary layer at $X = 0.06$ m and $X = 0.90$ m under different free stream turbulence intensities are shown in Fig. 6(a) and (b). As for the velocity profile, the increase in turbulence intensity leads to the formation of a "wake region" in the temperature profile which is all the more pronounced as the Tu_∞ and Reynolds numbers increase. This phenomenon is accompanied by a large increase in the thickness of the temperature boundary layer. As soon as $Tu_\infty \geqslant 12\%$ and $X > 0.06$ m, the thickness of the thermal boundary layer is more than three-fold the value of δ_t calculated from relation (1) using Blasius thickness for δ_v. However the thickening of the boundary layer is always less pronounced for the temperature layer than for the velocity layer. For example, for $Tu_\infty \approx 50\%$ and $Re_x = 126\,900$, the thickness of the velocity boundary layer is 60 mm while the thickness of the temperature layer is 45 mm. On the contrary, the increase of the slope of the near wall profile is more pronounced inside the thermal boundary layer than inside the velocity

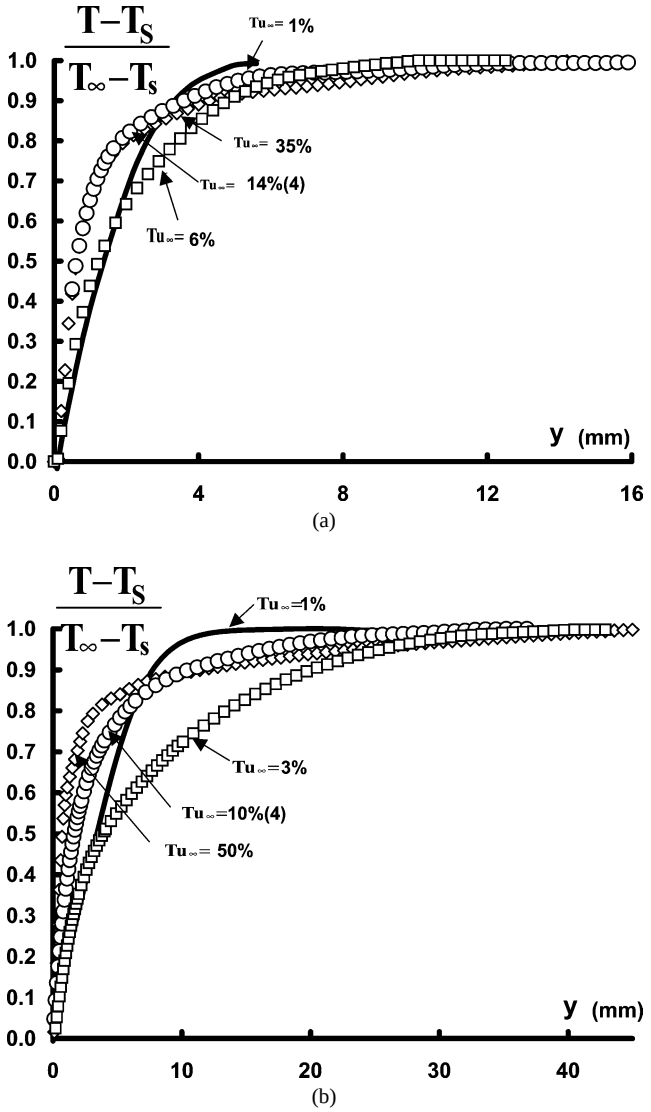

Fig. 6. Variation of the temperature profile with Tu_∞ at: (a) $X = 0.20$ m, (b) $X = 0.90$ m. Symbols are the same as in Fig. 2.

boundary layer. This large increase in the slope of the temperature profile expresses a strong increase in the heat transfer coefficient value. Heat transfer coefficients have been calculated from the slopes of temperature profiles (Table 2). Calculations of slopes in the near-wall region are very sensitive both to errors on the exact location of the wall and to the choice of the points which are considered to be in the linear part of the curve. The slopes were calculated taking into account the uncertainty on the wall location and different numbers of points. Effect of these uncertainties on the calculated slope and thus on the determination of the heat transfer coefficient was on average $+/-15\%$ of the given results. The effect of a variation of Tu_∞ on heat transfer coefficient increases as Re_x increases. For $Tu_\infty \approx 50\%$ and $Re_x = 126\,900$, the slope of the transfer coefficient value is more than three fold its value for $Tu_\infty \approx 1\%$ (Table 2).

Table 2
Heat transfer coefficient values ($W{\cdot}m^{-2}{\cdot}K^{-1}$) as a function of Tu_∞ calculated from the slope of the thermal profiles at three different distances from the promoters

Flow turbulence	Distance from the leading edge [m]		
	0.2	0.4	0.9
Blasius	6.9	5.1	3.1
$Tu_\infty = 1\%$	8.9	8.7	4.9
$Tu_\infty = 6\%$	11.5	11.7	5.1
$Tu_\infty = 12\%$	22.0	18.9	10.7
$Tu_\infty = 40$–50%	20.5	23.5	17.6

The joint increase of the slope of the thermal profile and the formation of a "wake region" leads to variations of $\delta_t{}^*$ and δ_t^{**} with Tu_∞ which are not as regular as in the case of the velocity boundary layer.

The less pronounced thickening of the thermal boundary layer with Tu_∞ in comparison with the velocity boundary layer seems to contradict the results of Péneau et al. [17]. The apparent contradiction between calculated and experimental results is probably due to the different starting conditions of development of the thermal boundary layer. In the calculations made by Péneau et al., thermal and velocity boundary layers start at the same points. Thus even when the free stream is laminar, the thermal boundary layer is already slightly thicker than the velocity boundary layer ($Pr = 0.7$). On the contrary, in the present experiments in a laminar free stream, the thermal boundary layer remained much thinner than the velocity boundary layer up to $X = 0.5$ m, due to the unheated starting length. Along this upstream length ($X < 0.5$ m) the thermal boundary which was "inside" the velocity boundary layer was not directly affected by the turbulence being so far isothermal.

This supports our previous remark on the necessity to take into account the "upstream history" of the development of the thermal boundary layer to understand the effect of free stream turbulence (see discussion in [5]). More work is needed to compare the effect of turbulence on the thermal and velocity boundary layers taking into account this "upstream history".

3.4. Measurements of the fluctuating velocity inside the boundary layer

The measured root mean square of the velocity fluctuation u' divided by the free stream velocity is displayed for two Reynolds numbers: $Re_x = 8460$ and 126 900 in Fig. 7.

Values of Tu measured for $Re_x = 8460$ are very similar to those obtained by Dyban and Epik for $Re_x = 6200$ (Fig. 7(a)). The level of Tu inside the boundary layer increases with Tu_∞. For $Tu_\infty \approx 1\%$, the value of Tu remains constant until $\eta \geqslant 4$ decreases afterwards regularly down to the wall. For $Tu_\infty = 6\%$, a clear maximum of Tu is observed inside the boundary layer located at $\eta \approx 3$. For $Tu_\infty \approx 14$–16%, this maximum is still located at $\eta \approx 3$ but is less pronounced. Moreover the curves obtained under

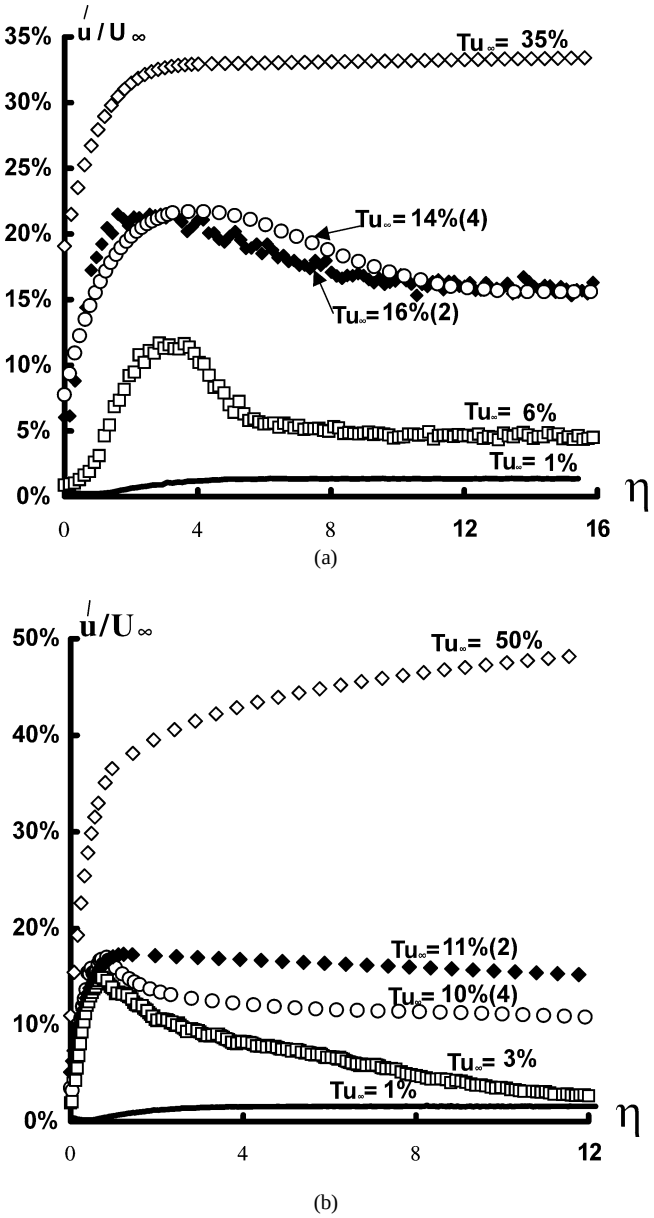

Fig. 7. Root mean square velocity profile inside the boundary layer divided by the free stream air velocity (*Tu*). (a) $Re_x = 8460$; full line, $Tu_\infty = 1\%$: white squares, $Tu_\infty = 6\%$; white dots, $Tu_\infty = 14\%$, promoter N°4 upstream contraction area; black diamonds, $Tu_\infty = 16\%$, promoter N°2 downstream contraction area; white diamonds, $Tu_\infty = 35\%$. (b) $Re_x = 126\,900$; full line, $Tu_\infty = 1\%$: white squares, $Tu_\infty = 3\%$; white dots, $Tu_\infty = 10\%$, promoter N°4 upstream contraction area; black diamonds, $Tu_\infty = 11\%$, promoter N°2 downstream contraction area; white diamonds, $Tu_\infty = 50\%$.

the two different turbulent scales are similar. For $Tu_\infty \approx 35\%$, there is no maximum of *Tu* which remains constant until $\eta \approx 3$ and decreases afterwards sharply towards the wall. Disappearance of a maximum value of *Tu* inside the boundary layer for $Tu_\infty \geqslant 20\%$ was also observed by Dyban and Epik [15].

For $Re_x = 126\,900$, the variations of *Tu* are similar to those observed for $Re_x = 6200$ (Fig. 7(b)). However the maximum *Tu* is located closer to the wall ($\eta \approx 1$) and the two curves obtained for $Tu_\infty \approx 11\%$ are different depending on the upstream turbulent scale. Moreover for $Tu_\infty \approx 50\%$, the value *Tu* seems to decrease slightly from the outside of the boundary layer until $\eta \approx 1$ before decreasing sharply towards the wall. It is also worth noticing that the maximum value obtained for $Tu_\infty = 3\%$ is very high and close to that obtained for $Tu_\infty \approx 11\%$. The value of this maximum cannot be connected with the local value of $Tu_\infty = 3\%$ and is probably explained by the upstream situation where the boundary layer is subjected to a free stream turbulence intensity of 6%.

4. Conclusion

Flat-plate boundary layers which develop under high free stream turbulence levels at moderate Reynolds numbers cannot be described using the two classical patterns of "laminar boundary layer" and "turbulent boundary layer". As already assumed in a previous paper [5], at moderate Reynolds numbers an increase in the free stream turbulence does not lead merely to rapid transition from the laminar boundary layer pattern to the turbulent boundary pattern. New boundary layer structures develop features which are intermediate between the two well known patterns.

When $Tu_\infty \approx 1\%$, the average velocity profile inside the boundary layer can be described by the Blasius solution even if the boundary layer is 10–15% thicker and if there is already penetration or production of turbulent fluctuations inside that layer. For $Tu_\infty \geqslant 6\%$, the velocity boundary layer thickens a lot with the free stream turbulence intensity as well as the displacement and momentum thicknesses. A "wake region" appears in the profile which can be affected, if the boundary layer is thick ($Re_x = 126\,900$, $Tu_\infty \approx 12\%$), by the turbulence integral scale. Experimental results obtained for $Tu_\infty = 6$–12% are very close to those calculated by large eddy simulations for $Tu_\infty = 10\%$ [17]. They also confirm the production of turbulent energy inside the boundary layer. In the present experiments, the effect of very high free stream turbulence intensities were investigated. Our results show that for $Tu_\infty = 30$–50% the thickening of the velocity boundary layer and the turbulence production or penetration inside that layer goes on even if it seems to be less intensive than for Tu_∞ between 1 and 12%.

One of the main objectives of the present study was to compare the effect of free stream turbulence on the thermal boundary layer in relation to the effect on the velocity boundary layer. As for the velocity boundary layer, an increase of free stream turbulence thickens the thermal boundary layer, it introduces a "wake region" in the "outside" temperature profile and it increases the slope of the near-wall profile. This increase of slope is much more pronounced for the temperature than for the velocity profile, while, contrary to what was observed by LES, the thickening of the boundary layer is less pronounced for the thermal

layer than for the velocity layer. This slower thickening of the thermal boundary layer is probably due to the existence of an unheated starting length in our experimental device. Unheated starting lengths are commonly encountered in practical situations. Thus they cannot be overlooked when transposing results obtained on the velocity boundary layer to the thermal boundary layer.

Acknowledgements

The authors thank Annik Lacombe and Christine Young (UCDIST Jouy) for proof reading and correction of the English.

References

[1] A. Kondjoyan, J.D. Daudin, Etat des connaissances sur les coefficients de transferts de chaleur et de matière à l'interface air–solide pour un objet isolé lisse, Entropie 30 (1994) 3–16.
[2] A. Kondjoyan, J.D. Daudin, Effects of free stream turbulence intensity on heat and mass transfers at the surface of a circular cylinder and an elliptical cylinder, axis ratio 4, Internat. J. Heat Mass Transfer 38 (1995) 1735–1749.
[3] A. Kondjoyan, J.D. Daudin, Heat and mass transfer coefficients at the surface of a pork hindquarter, J. Food Engng. 32 (1997) 225–240.
[4] L. Ghisalberti, A. Kondjoyan, Convective heat transfer coefficients between air flow and a short cylinder- Effect of air velocity and turbulence. Effect of body shape, dimensions and position in the flow, J. Food Engng. 42 (1999) 33–44.
[5] A. Kondjoyan, F. Péneau, H.C. Boisson, Effect of high free stream turbulence on heat transfer between plates and air flows: A review of existing experimental results, Internat. J. Therm. Sci. 41 (2002) 1–16.
[6] G. Charnay, G. Comte-Bellot, J. Mathieu, Development of a turbulent boundary layer on a flat plate in an external turbulent flow, AGARD, 1971, Paper N°27.
[7] P. Bradshaw, Effect of free-stream turbulence on turbulent shear layers. Aero. Report 74-10, Imperial College of Science and Technology, Department of Aeronautics, London, October 1974.
[8] J.C. Simonich, P. Bradshaw, Effect of free-stream turbulence on heat transfer through a turbulent boundary layer, J. Heat Transfer 100 (1978) 671–677.
[9] M.F. Blair, Influence of free-stream turbulence on turbulent boundary layer heat transfer and mean profile development, part I-Experimental data, J. Heat Transfer 105 (1983) 33–40.
[10] M.F. Blair, Influence of free-stream turbulence on turbulent boundary layer heat transfer and mean profile development, part II-Analysis of the results, J. Heat Transfer 105 (1983) 41–47.
[11] P.E. Hancock, P. Bradshaw, The structure of a turbulent boundary layer beneath a turbulent free stream, Sixth Symposium on Turbulent Shear Flows, Toulouse, France, 1987, Paper 1.1.
[12] P.K. Maciejewski, R.J. Moffat, Heat transfer with very high free-stream turbulence: Part I—Experimental data, J. Heat Transfer 114 (1992) 827–833.
[13] J. Kestin, P.F. Maeder, H.E. Wang, Influence of turbulence on the transfer of heat from plates with and without a pressure gradient, Internat. J. Heat Mass Transfer 3 (1961) 133–154.
[14] G.H. Junkhan, G.K. Serovy, Effects of free-stream turbulence and pressure gradient on flat-plate boundary-layer velocity profiles and on heat transfer, J. Heat Transfer (1967) 169–176.
[15] E.P. Dyban, E.Ya. Epik, Transferts de chaleur et hydrodynamique dans les écoulements rendus turbulents, in: Monographie Traduite du Russe par l'I.N.R.A., Naukova Dumka, Kiev, 1985.
[16] W.S. Saric, H.L. Reed, E.J. Kerschen, Boundary-layer receptivity to freestream disturbances, Annual Rev. Fluid Mech. 34 (2002) 291–319.
[17] F. Péneau, H.C. Boisson, A. Kondjoyan, N. Djilali, Flat plate boundary layer spatial structuration under a free-stream turbulence, Internat. J. Comput. Fluid Dynam. 18 (2004) 175–188.
[18] F. Peyrin, A. Kondjoyan, Effect of turbulent integral length scale on heat transfer around a circular cylinder placed cross to an air flow, Exp. Therm. Fluid Sci. 26 (2002) 455–460.
[19] H.H. Bruun, Hot-Wire Anemometry—Principles and Signal Analysis, Oxford Science Publications, Oxford, 1995.
[20] W.M. Kays, M.E. Crawford, Convective Heat and Mass Transfer, second ed., McGraw-Hill, New York, 1980.
[21] H. Schlichting, Boundary Layer Theory, seventh ed., in: Classic Textbook Reissue Series, McGraw-Hill, New York, 1951.